

# Optimisation of lignin liquefaction with polyethylene glycol/ glycerol through response surface methodology modelling

Fabio Hernández-Ramos<sup>a</sup>, Vincent Novi<sup>b</sup>, María González Alriols<sup>a</sup>, Jalel Labidi<sup>a</sup>, Xabier Erdocia<sup>c,\*</sup>

<sup>a</sup> Biorefinery Processes Research Group (BioRP), Chemical and Environmental Engineering Department, University of the Basque Country (UPV/EHU), Plaza Europa 1, 20018 San Sebastian, Spain

<sup>b</sup> École Nationale Supérieure de Chimie de Lille, Avenue Mendeleiev, Bât. C7, 90108 Lille, France

<sup>c</sup> Biorefinery Processes Research Group (BioRP), Department of Applied Mathematics, University of the Basque Country (UPV/EHU), Rafael Moreno "Pichichi" 3, Bilbao 48013, Spain

## ARTICLE INFO

### Keywords:

Lignin  
Bio-polyol  
Liquefaction  
Response surface methodology

## ABSTRACT

In order to diminish the dependence on oil lignin, which is the most abundant biopolymer of phenolic origin on Earth and can be utilised in different industrial endeavours, such as, the production of polyurethanes. In this study, hardwood (*Eucalyptus globulus*) and softwood (*Pinus radiata*) organosolv lignins were employed to produce bio-polyols through microwave-assisted liquefaction. The resulting bio-polyols possessed specific properties to be employed in the synthesis of rigid and elastic polyurethanes. The values of the reaction parameter were optimized using response surface methodology to determine the most effective conditions for producing bio-polyols from both types of lignins for the purpose of rigid and elastic polyurethane formulation. The effect of catalyst concentration (%wt.), temperature (°C) and Polyethylene glycol/Glycerol weight ratio on the molecular weight ( $M_w$ ) and hydroxyl number ( $I_{OH}$ ) of bio-polyols was evaluated. The optimum reaction conditions of bio-polyols production for rigid polyurethanes were virtually equal for the two lignins, 159–161 °C, Polyethylene glycol/Glycerol ratio of 3 without catalyst. On the contrary, the bio-polyols for elastic polyurethanes required different reaction parameters depending on the lignin used. For hardwood lignin the optimised conditions were 180 °C, 7.57 (Polyethylene glycol/Glycerol ratio) and 5.00% of catalyst while for softwood lignin were 160 °C, 7.34 (Polyethylene glycol/Glycerol) and 3.85% of catalyst. Additionally, the bio-polyols obtained at optimised conditions were fully characterised and acid number, polydispersity index, functionality and the rheological behaviour was studied.

## 1. Introduction

In 1937 Dr. Otto Bayer synthesised for the first time one of the most versatile synthetic materials created by humans (Hai et al., 2021). Such materials, known as polyurethanes (PU), are generally synthesised by polyaddition reactions between isocyanates and polyols to produce linear or crosslinked polymeric materials (Lambeth, 2021) including foams, elastomers, composites, paints, coatings and adhesives (Gomez-Lopez et al., 2021). The polyols market generated approximately USD 26.2 billion per year in 2019 and the business is expected to grow to USD 34.4 billion per year by 2024 (Perez-Arce et al., 2020). Generally, polyols employed in PU synthesis are derived from fossil resources. However, in recent years, due to increased environmental awareness and

more rigorous legislation, the use of lignocellulosic biomass as a platform for producing sustainable polyols is gaining relevance (Gómez-Jiménez-Aberasturi and Ochoa-Gómez, 2017).

Lignin is one of the main components of lignocellulosic biomass and is considered the most abundant renewable phenolic polymer on Earth (Laurichesse and Avérous, 2014). Nowadays, lignin is mainly generated as a by-product in pulp and paper industry and in second generation biorefineries. Therefore, it is a low cost and highly available product, which is actually used as fuel to supply the energy needs of the industrial plant (Erdocia et al., 2021). Lignin is an aromatic biopolymer formed through the union of three monolignols called sinapyl alcohol, coniferyl alcohol and *p*-coumaryl alcohol mainly via ether ( $\beta$ -O-4) and C-C bonds (Erdocia et al., 2014) which conforms a three-dimensional structure rich

\* Corresponding author.

E-mail address: [xabier.erdocia@ehu.eus](mailto:xabier.erdocia@ehu.eus) (X. Erdocia).

<https://doi.org/10.1016/j.indcrop.2023.116729>

Received 1 March 2022; Received in revised form 11 March 2023; Accepted 13 April 2023

Available online 18 April 2023

0926-6690/© 2023 The Author(s). Published by Elsevier B.V. This is an open access article under the CC BY-NC-ND license (<http://creativecommons.org/licenses/by-nc-nd/4.0/>).

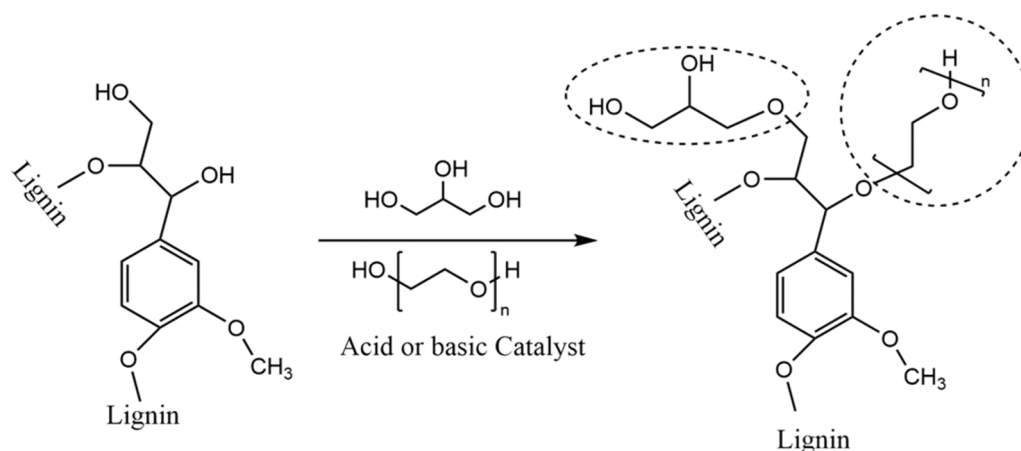


Fig. 1. Schematic reaction of lignin liquefaction reaction employing PEG and glycerol as solvents.

in phenolic and aliphatic hydroxyl groups that make lignin suitable for polyol synthesis (Kühnel et al., 2015). Lignin can be directly used in the polymer industry, although, without modification, it can be used only in small quantities, due to its thermal degradation, mechanical properties, and low reactivity (Laurichesse and Avérous, 2014). Among others, liquefaction with polyhydric alcohols is one of the most widely used technologies to produce polyols from lignocellulosic biomass (Xue et al., 2015). In this process (Fig. 1) lignin is depolymerised through solvolytic reactions creating smaller and more reactive fragments which can repolymerise or react with the liquefaction agents forming viscous liquid rich in hydroxyl groups (Hu et al., 2014).

Conventional lignin liquefaction process is carried out under atmospheric pressure using polyhydric alcohols as liquefaction solvents and can be either acid or base catalysed, although the most used catalyst is sulphuric acid (da Silva et al., 2019). Under acidic conditions, the temperature of the reaction ranges between 150 and 170°C and the reaction time is around 90 min (Hu et al., 2014). However, under these acidic conditions, lignin repolymerisation reactions are favoured, decreasing the yield of the reaction. Besides the effect of the catalyst, the yield can also be influenced by high temperatures, high residence times and the solvent-to-biomass ratio (Hu et al., 2014). Therefore, since traditional lignin liquefaction processes require elevated energy cost due to the long residence times and elevated temperatures, it is necessary to explore new and more environmentally friendly alternatives to reduce these operational costs and to optimise the abovementioned variables to improve the industrial viability of the process. In this sense, the use of microwave-assisted irradiation is an interesting alternative to conventional lignin liquefaction methods, since it allows faster and more homogeneous heating while reducing the reaction time and, therefore, decreasing the energy consumption (Nde et al., 2021). Different studies have been carried out in recent years about the liquefaction of different lignin types through microwave-assisted irradiation, resulting in bio-polyols suitable for PU manufacture (Cinelli et al., 2013; da Silva et al., 2019, 2017; Gosz et al., 2018; Sequeiros et al., 2013; Xue et al., 2015; Tran et al., 2021).

In the present study, the optimisation of the liquefaction reaction conditions using microwave irradiation technology to obtain suitable bio-polyols for both, the manufacture of rigid and elastic PU is proposed. Two different organosolv lignins, obtained from *Eucalyptus globulus* and *Pinus radiata*, which were previously fractionated through ultrasonication, were employed. The optimisation was carried out using a Box-Behnken experimental design through response surface methodology and the effect of the independent variables on the molecular weight ( $M_w$ ) and hydroxyl number ( $I_{OH}$ ) of bio-polyols was studied. Other parameters, such as polydispersity index (PDI), functionality ( $f$ ) and acid number ( $A_n$ ) of optimised bio-polyols were also discussed, as well as their thermal degradation and rheological behaviour.

## 2. Materials and methods

### 2.1. Materials

*Eucalyptus globulus* and *Pinus radiata* were obtained from Papelera Guipuzcoana Zikuñaga S.A. and Ebaki XXI S.A., respectively. Both companies are located in the Basque Country in Spain. Ethanol used for the organosolv treatment was purchased from Scharlab S.L. Sulphuric acid (96%), polyethylene glycol 400 (PEG) and glycerol (Gly) were obtained from Panreac. Fisher Scientific supplied the ethyl acetate (HPLC grade), sodium sulphate anhydrous ( $\geq 99\%$ ), dimethylformamide (DMF, for HPLC  $\geq 99.9\%$ ), lithium bromide, 1,4-dioxane, pyridine (analytical grade) and phthalic anhydride (98%).

### 2.2. Lignin obtaining procedure

In order to obtain the lignin samples from *Eucalyptus globulus* and *Pinus radiata* sawdust, both raw materials were first subjected to an organosolv delignification process employing the reaction conditions described in our previous work (Hernández-Ramos et al., 2021), which are summarised below, a 1.5 L stainless 5500 steel Parr reactor equipped with a 4848 Parr controller was employed. A 50% EtOH (w/w) solution and a reaction time of 75 min were used for both *Eucalyptus globulus* and *Pinus radiata* delignification reactions. However, different temperatures and solid/liquid ratios were employed. Thus, in the case of *Eucalyptus globulus*, the reaction was carried out at 200°C and a solid to liquid ratio of 1:6, while the delignification of *Pinus radiata* was conducted at 210°C and a solid to liquid ratio of 1:8. Afterwards, the organosolv black liquors were separated from the pulp using vacuum filtration. Then, to reduce the molecular weight and polydispersity index of the dissolved lignins contained in the black liquors, these were submitted to an ultrasonication process. To do so, a HD 3100 Sonoplus ultrasonic homogenizer was employed under the following conditions: 60 min, 35°C and 35% of output amplitude (Wells et al., 2013). Finally, the pH of the black liquors was adjusted with acidified water (pH 2) to precipitate the dissolved lignin. This resulted in a solid phase (lignin) and an aqueous phase, which were separated by membrane filtration using a 2 L stainless steel holder and a 0.22  $\mu\text{m}$  pore diameter nylon filter.

### 2.3. Lignin characterisation

Lignin obtained before and after ultrasound treatment was analysed by gel permeation chromatography (GPC) and FTIR spectroscopy to verify the diminution of the molecular weight and to determine possible variations in the chemical structure. For the former, a JASCO instrument equipped with an LC.NetII/ADC interface, two columns in series (PolarGel-M 300 mm  $\times$  7.5 mm) and a RI-2031Plus refractive index

**Table 1**  
Experimental variables involved in the study.

Variable	Definition	Units	Nomenclature	Value
Fixed	Time	min		5
	SLR <sup>a</sup>	(w/w)		1/6
Independent	Catalyst	(% wt.)	Cat	0–5
	Temperature	°C	Temp	140–180
	PEG/Gly ratio	(w/w)	PEG/Gly	3–9
Dependents	Molecular weight	g/mol	M <sub>w</sub>	
	Hydroxyl number	mg KOH/g	I <sub>OH</sub>	

<sup>a</sup> Solid to liquid ratio (SLR).

detector was used. N,N-dimethylformamide with 1% lithium bromide was employed as mobile phase with a flow rate of 700 mm<sup>3</sup>/min and a temperature of 40°C was used. The calibration curve was made employing polystyrene standards with molecular weight from 266 to 70,000 g/mol (Sigma-Aldrich). For the latter, a PerkinElmer Spectrum Two FT-IR Spectrometer equipped with a Universal Attenuated Total Reflectance accessory provided with an internal reflection diamond crystal lens was employed. 20 scans in transmission mode were collected with a resolution of 4 cm<sup>-1</sup> in the range of 4000–400 cm<sup>-1</sup>.

## 2.4. Experimental design of microwave assisted lignin liquefaction

### 2.4.1. Microwave assisted lignin liquefaction procedure

Liquefaction reaction of lignin in presence of PEG, Gly and catalyst (H<sub>2</sub>SO<sub>4</sub>) was performed in a CEM Microwave Discover System Model with a temperature controller instrument and an internal temperature sensor. The reaction was carried out under constant stirring and the residence time was 5 min for all the reactions. As soon as the reaction time finished, the reactor cooling system was activated to cool the vessel until 50 °C. Then the vessel was introduced into a recipient with cold water to reach a safe handling temperature. Once cooled, the content of the vessel was diluted employing acetone and filtered under vacuum to remove the unreacted solids. Finally, the acetone was evaporated at 50 °C under vacuum.

### 2.4.2. Experimental design

A response surface methodology (RSM) was used to determine the effect of the independent variables: Catalyst concentration (%wt.) (Cat), Temperature (°C) (Temp) and PEG/Gly ratio (%wt.) on the molecular weight (M<sub>w</sub>) and I<sub>OH</sub> of bio-polyols. A three block Box-Benken Design (BBD), which consisted in 15 experiment, with three central point was selected for the experimental design and optimisation.

A second-order polynomial equation (Eq. 1) was used to fit the experimental data:

$$y = b_0 + \sum_{i=1}^3 b_i x_i + \sum_{i < j = 2}^3 b_{ij} x_i x_j + \sum_{i=1}^3 b_{ii} x_i^2 + \varepsilon \quad (1)$$

where  $y_j$  represent de dependent variables (M<sub>w</sub> and I<sub>OH</sub>),  $b_0$ ,  $b_i$ ,  $b_{ij}$ ,  $b_{ii}$  correspond to the regression coefficients estimated from the experimental results employing the least-squares method,  $x_i$  and  $x_j$  are the dimensionless normalized independent variables Cat, Temp and PEG/Gly, with a variation range from – 1 to 1.

Through the evaluation of the lack of fit, the R<sup>2</sup> determination coefficient, the significance of the regression coefficients and the F-test value obtained from the analysis of variance, the suitability of the model was validated. The experimental design, statistical analysis and regression model were generated employing the Statgraphics Centurion version XVI (Statpoint Technologies Inc., Warrenton, VA, USA). Optimal conditions to produce polyols for rigid and elastic PU, predicted by the desirability function of the abovementioned software, were obtained by adjusting the dependent variables M<sub>w</sub> and I<sub>OH</sub>. Microsoft Excel's Data Analysis Add-In, USA, was employed to fit the experimental data. Model validation was carried out by performing a triplicate of each experiment

**Table 2**

M<sub>w</sub> (g/mol), M<sub>n</sub> (g/mol) and PDI of organosolv lignins and ultrasonicated organosolv lignins.

Sample	M <sub>w</sub> (g/mol)	M <sub>n</sub> (g/mol)	PDI
EL	3632	952	3.81
EUL	2837	888	3.20
PL	3529	1035	3.41
PUL	2924	911	3.21

under optimal conditions and comparing them with the values predicted by the model.

The experimental variables considered in this study (Table 1), include the fixed variables, the independent variables, as well as the dependent ones including the corresponding variation ranges of each variable.

### 2.4.3. Characterisation of the obtained bio-polyols

Bio-polyols were analysed to determine the molecular weight distribution (M<sub>w</sub>, M<sub>n</sub> and M<sub>w</sub>/M<sub>n</sub>) as well as the I<sub>OH</sub>. For the determination of the molecular weight distribution, gel permeation chromatography was employed following the procedure described in Section 2.3.

The I<sub>OH</sub> (mg KOH/g of sample) and the acid number (mg KOH/g of sample) of bio-polyols were determined employing the ASTM D4274 (Methods, 2000) and ASTM D974 (ASTM, 2013) standards, respectively. The reaction for the determination of the I<sub>OH</sub> consisted in 0.5–1 g of bio-polyol dissolved into 25 mL of a phthalate reagent (115 g phthalic anhydride dissolved in 700 mL of pyridine prepared 24 h earlier to the determination of I<sub>OH</sub>) at 115°C for 1 h under reflux and constant stirring. After the reaction time, 50 mL of pure pyridine were added through the condenser. Finally, the solution was back titrated employing a 0.5 M NaOH solution. On the other hand, 0.4 g of bio-polyol was dissolved in 50 mL of a solvent mixture composed by 1,4-dioxane:water (4:1 v/v) and back titrated with a 0.1 M KOH solution in ethanol. Nevertheless, due to the dark colour of the bio-polyols, an evident colour change was difficult to observe by using phenolphthalein as indicator in the titration. Therefore, a potentiometric titration was performed to detect the equivalent point employing an automatic titrator 888 (Titrande Metrohm) and Tiamo 2.5 software.

### 2.4.4. Characterisation of bio-polyols at the optimised reaction conditions

To validate the model, experiments were triplicated under the optimal conditions and the results (M<sub>w</sub> and I<sub>OH</sub> values) were compared with the theoretical ones. Once the model was validated, the bio-polyols obtained under the optimal conditions were further characterised to determine relevant parameters, such as the chemical structure, the thermal degradation, and the rheological behaviour.

A thermogravimetric analysis (TGA) was employed to determine the thermal degradation of bio-polyols. Briefly, 5 mg of bio-polyol were heated from 25°C to 800°C under inert atmosphere (N<sub>2</sub> 10 mL·min<sup>-1</sup>) and 10 °C min<sup>-1</sup> heat rate in a TGA/SDTA RSI analyser (Mettler Toledo).

The synthesized bio-polyols were submitted to a rotational test to analyse their rheological behaviour employing a Haake Viscotester IQ (Thermo Fisher Scientific). The rotational test was performed to determine the viscosity ( $\eta$ ) and the shear stress ( $\tau$ ) as a function of the shear rate ( $\dot{\gamma}$ ). Tests were performed at room temperature employing a coaxial cylinders geometry (CC 25 DIN/Ti adapter), with 12.54 mm piston radius and 1.00 mm ring gap. The employed shear rate sweep was from 0.02 to 120 s<sup>-1</sup>.

## 3. Results and discussion

### 3.1. Lignin characterisation

Since lignins with low molecular weight are desired to produce polyols (Li et al., 2015a), the obtained *Eucalyptus globulus* and *Pinus*

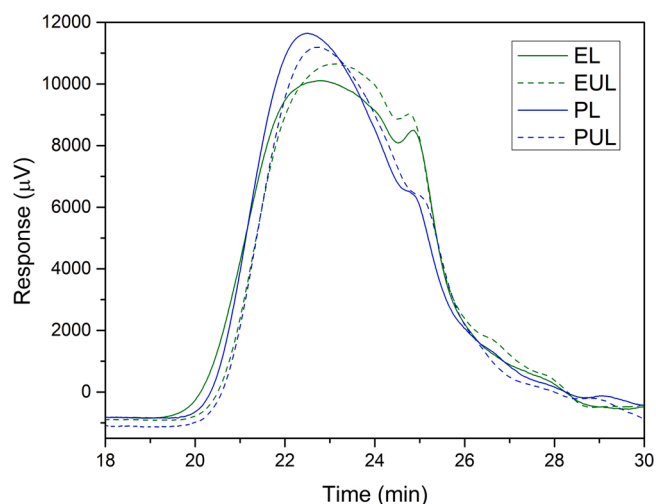


Fig. 2. Molecular weight distribution of organosolv lignins and ultrasonicated organosolv lignins.

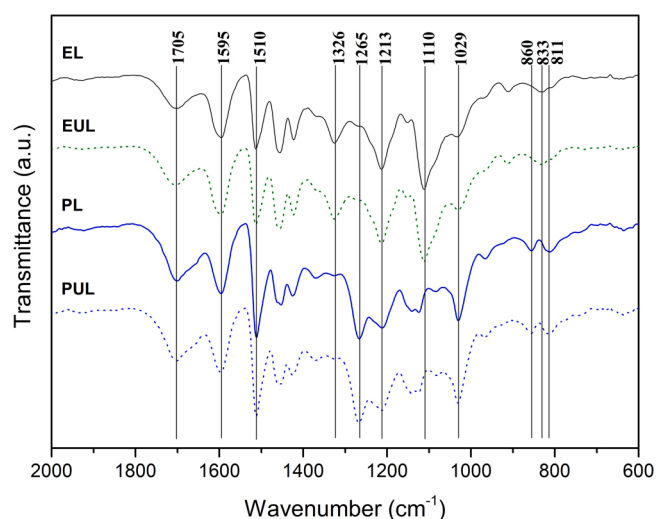


Fig. 3. Fingerprint region of FTIR spectra of non-ultrasonicated and ultrasonicated organosolv lignins.

Table 3

Independent normalised and not normalised variables, Cat (%wt.) ( $X_1$ ); Temperature ( $^{\circ}\text{C}$ ) ( $X_2$ ) and PEG/Gly (w/w) ( $X_3$ ), together with the dependent variables, average molecular weight ( $Y_{Mw}$ ) and hydroxyl number ( $Y_{IOH}$ ), of the Box-Behnken experimental design.

Exp	Independent variables						Dependent variables			
	Not normalised variables			Normalised Variables			<i>Eucalyptus globulus</i>		<i>Pinus radiata</i>	
	Cat (% wt.)	Temp ( $^{\circ}\text{C}$ )	PEG/Gly (w/w)	$X_1$	$X_2$	$X_3$	$Y_{Mw}$ (g/mol)	$Y_{IOH}$ (mgKOH/g)	$Y_{Mw}$ (g/mol)	$Y_{IOH}$ (mgKOH/g)
1	2.5	180	9	0	1	1	3532	273.0	3576	211.3
2	2.5	160	6	0	0	0	2904	311.5	5469	294.0
3	0	180	6	-1	1	0	1752	221.5	1710	330.5
4	2.5	180	3	0	1	-1	3753	562.9	4896	592.6
5	2.5	140	9	0	-1	1	2169	243.0	4012	320.9
6	5	180	6	1	1	0	5926	290.1	4594	382.8
7	0	140	6	-1	-1	0	1662	260.9	1461	329.9
8	5	160	3	1	0	-1	3854	688.2	5136	551.9
9	2.5	160	6	0	0	0	3005	262.6	4469	232.4
10	2.5	140	3	0	-1	-1	2269	484.9	2922	456.7
11	5	160	9	1	0	1	3623	223.7	4116	194.2
12	2.5	160	6	0	0	0	2700	289.9	4077	247.0
13	0	160	9	-1	0	1	1637	326.2	1497	353.8
14	0	160	3	-1	0	-1	1771	644.8	1372	457.5
15	5	140	6	1	-1	0	3472	247.9	3991	262.3

*radiata* organosolv lignins (EL and PL) were ultrasonicated. These ultrasonicated lignins, called EUL and PUL from the ultrasonication of EL and PL respectively, showed lower molecular weight than the originals as summarised in Table 2. In both cases, similar molecular weight reduction was achieved with respect to the original lignins. Concretely, a 21.8% reduction in the case of EUL and 17.1% for PUL. The molecular weight reduction, although considerable, was far from that obtained by Wells et al. (2013), who obtained a reduction of 85.9% under the studied conditions. This difference could be due to a lower effect of cavitation because of the employed equipment. This decrease in the molecular weights can be observed in Fig. 2 since the chromatograms corresponding to the ultrasonicated lignins (EUL and PUL) exhibited lower retention times than the original ones.

FTIR spectroscopy was employed to characterise lignins to confirm that their chemical structure was not altered during the ultrasound fractionation process. As can be seen in Fig. 3, no differences were observed between lignin samples from the same raw material before and after being subjected to the ultrasonication process. Thus, it can be concluded that the ultrasound process did not produce any changes in the chemical structure of the lignins.

As can be observed the fingerprint region of the FTIR spectra (Fig. 3) showed the characteristic bands of lignin. In all samples a broad peak ( $3415\text{ cm}^{-1}$ ) corresponding to OH stretching of phenolic units is observed. The vibration of aliphatic CH bonds was also visible at between  $2970\text{ cm}^{-1}$  and  $2840\text{ cm}^{-1}$ . The band of carbonyl group, the vibration of the aromatic skeleton plus CO stretching and the stretching of CC plus C-O plus C=O at  $1705\text{ cm}^{-1}$ ,  $1595\text{ cm}^{-1}$  and  $1213\text{ cm}^{-1}$  respectively appeared in all samples. Nevertheless, since hardwood lignins are generally composed by an equal proportion of S and G units, whereas softwood lignin is predominantly constituted by G units several differences could be observed between lignin from hardwood and softwood. Thus, the spectra of lignin from *Eucalyptus globulus* showed more intense signal in the peaks at  $1326\text{ cm}^{-1}$ ,  $1110\text{ cm}^{-1}$  and  $833\text{ cm}^{-1}$ . These bands correspond to the condensed S and G rings, the aromatic CH deformation of S units and to CH group out of plane in positions 2 and 6 in S units. On the other hand, in the case of lignin from *Pinus radiata*, the signals were more intense in the bands corresponding to the G units, i.e.: vibration of the aromatic ring in G units ( $1510\text{ cm}^{-1}$ ), G ring plus CO ( $1265\text{ cm}^{-1}$ ), aromatic CH in plane deformation of G units ( $1029\text{ cm}^{-1}$ ) and CH out of plane in position 2, 5 and 6 in G units ( $860\text{ cm}^{-1}$  and  $811\text{ cm}^{-1}$ ) (Chen et al., 2015).

**Table 4**  
Regression coefficient plus their statistical parameters.

Coefficients	<i>Eucalyptus globulus</i>		<i>Pinus radiata</i>	
	Y <sub>Mw</sub>	Y <sub>IOH</sub>	Y <sub>Mw</sub>	Y <sub>IOH</sub>
b <sub>0</sub>	2869.67 <sup>a</sup>	288.02 <sup>a</sup>	4671.67 <sup>a</sup>	257.78 <sup>a</sup>
b <sub>1</sub>	1256.63 <sup>a</sup>	-0.43	1474.63 <sup>a</sup>	-10.04
b <sub>2</sub>	673.88 <sup>a</sup>	13.85	298.75	18.42
b <sub>3</sub>	-85.75	-164.38 <sup>a</sup>	-140.63	-122.31 <sup>a</sup>
b <sub>12</sub>	591.00 <sup>b</sup>	20.40	88.50	29.96 <sup>c</sup>
b <sub>13</sub>	-24.25	-36.49	-286.25	-63.49 <sup>a</sup>
b <sub>23</sub>	-30.25	-11.99	-602.50 <sup>c</sup>	-61.37 <sup>a</sup>
b <sub>11</sub>	61.92	23.42	-1276.96 <sup>a</sup>	31.27 <sup>c</sup>
b <sub>22</sub>	271.42	-56.36 <sup>c</sup>	-455.71	37.30 <sup>c</sup>
b <sub>33</sub>	-210.33	159.27 <sup>a</sup>	-364.46	100.30 <sup>a</sup>
R <sup>2</sup>	0.97	0.97	0.96	0.98
R <sup>2</sup> -adjusted	0.92	0.90	0.87	0.95
F <sub>α=0.05</sub>			4.773	
F-exp	19.516	15.463	11.795	28.588
Area under F-exp	0.002	0.004	0.007	0.001
Significance level	99.779	99.618	99.287	99.911

<sup>a</sup> Significant coefficients at the 99% of confidence level.  
<sup>b</sup> Significant coefficients at the 95% of confidence level.  
<sup>c</sup> Significant coefficients at the 90% of confidence level.

**3.2. Optimisation of the conditions for obtaining suitable bio-polyols for PU applications**

In the present study, microwave-assisted irradiation method was employed. A response surface methodology in combination with a Box-Behnken design was employed to accomplish the optimisation of the bio-polyols obtaining reaction conditions. Statgraphic software was used to establish the experiments set, which is summarised in Table 3, as well as the experimental values that corresponded to the dependent variables (Y<sub>IOH</sub> and Y<sub>Mw</sub>).

Regarding Table 3, the I<sub>OH</sub> values ranged from 221.5 mgKOH/g (exp. 3) to 688.2 mgKOH/g (exp. 8) for *Eucalyptus globulus* bio-polyol, and from 211.3 mgKOH/g (exp. 1) to 592.6 mgKOH/g (exp. 4) for *Pinus radiata* bio-polyol. On the other hand, the average molecular weight (M<sub>w</sub>) ranged between 1637 g/mol (exp. 13) and 5692 g/mol (exp. 6) and between 1372 g/mol (exp. 14) and 5469 g/mol (exp. 2) for the bio-

polyols obtained from the liquefaction of lignin from *Eucalyptus globulus* and *Pinus radiata*, respectively.

In Table 4 the regression coefficients and their corresponding significance levels according to Student's t-test, as well as the R<sup>2</sup> determination coefficient, the adjusted R<sup>2</sup> and the statistical significance (Fisher's F-test) are summarised. F<sub>α=0.05</sub>, which is the value of the distribution that leaves an area behind the density function equal to 0.05 on its right (95% of significance level), was calculated employing the free software R (version 4.1.1) where the degrees of freedom are expressed through Eq. 2. On the other hand, the experimental F (F-exp) was determined using Eq. 3.

$$\text{Degrees of freedom} = K; n - (K + 1) \tag{2}$$

$$F = \frac{R^2 / K}{(1 - R^2) / [n - (K + 1)]} \tag{3}$$

where K is the number of model parameters, n is the number of data points and R<sup>2</sup> is the determination coefficient.

According to Table 4, the obtained R<sup>2</sup> determination coefficients were above 0.95 in all cases. Regarding the bio-polyol obtained from the liquefaction of *Eucalyptus globulus* lignin, R<sup>2</sup> of 0.97 was obtained for both M<sub>w</sub> and I<sub>OH</sub>, while for the polyol obtained from the liquefaction of *Pinus radiata* lignin these values were 0.96 for M<sub>w</sub> and 0.98 for I<sub>OH</sub>. This indicated that only a small number of total variations remained unexplained using the selected model, concretely 3% for the former and 4% and 2% for the latter. According with the obtained R<sup>2</sup> determination coefficients, it could be concluded that the model was appropriate to describe the interactions between the selected variables, since the R<sup>2</sup> determination coefficient indicate the validity of the design via the explanation of the total variations of the model (Morales et al., 2018). Furthermore, the predictivity of the model obtained through Fisher's F-test confirmed that the selected model was statistically relevant since the F-experimental values were higher than the F<sub>α</sub> values in all cases, which indicates that the models were statistically relevant above 95%. (Fernández-Marín et al., 2021).

Regression coefficients presented in Table 4 showed a different behaviour depending on the used raw material. Thus, X<sub>1</sub>, X<sub>2</sub> and the interaction X<sub>12</sub> were the most relevant independent variables for the

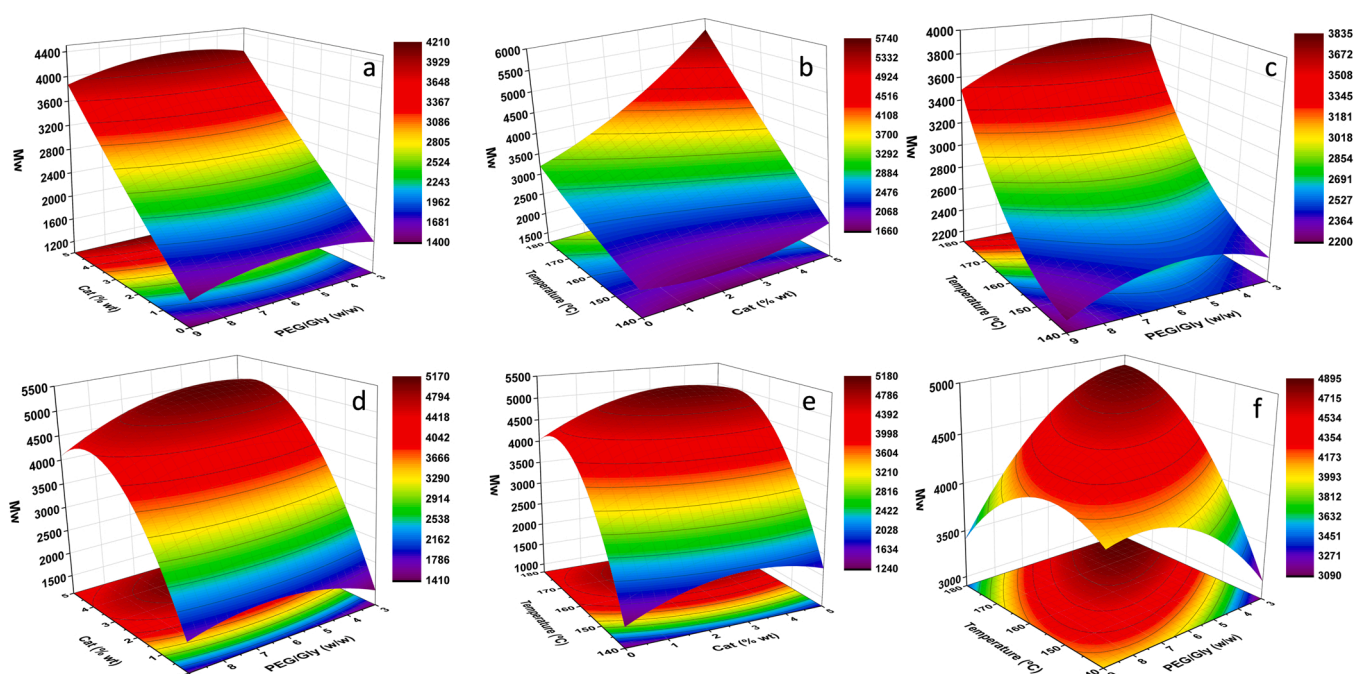


**Fig. 4.** Response surface for M<sub>w</sub>: *Eucalyptus globulus* (a, b, c); *Pinus radiata* (d, e, f).

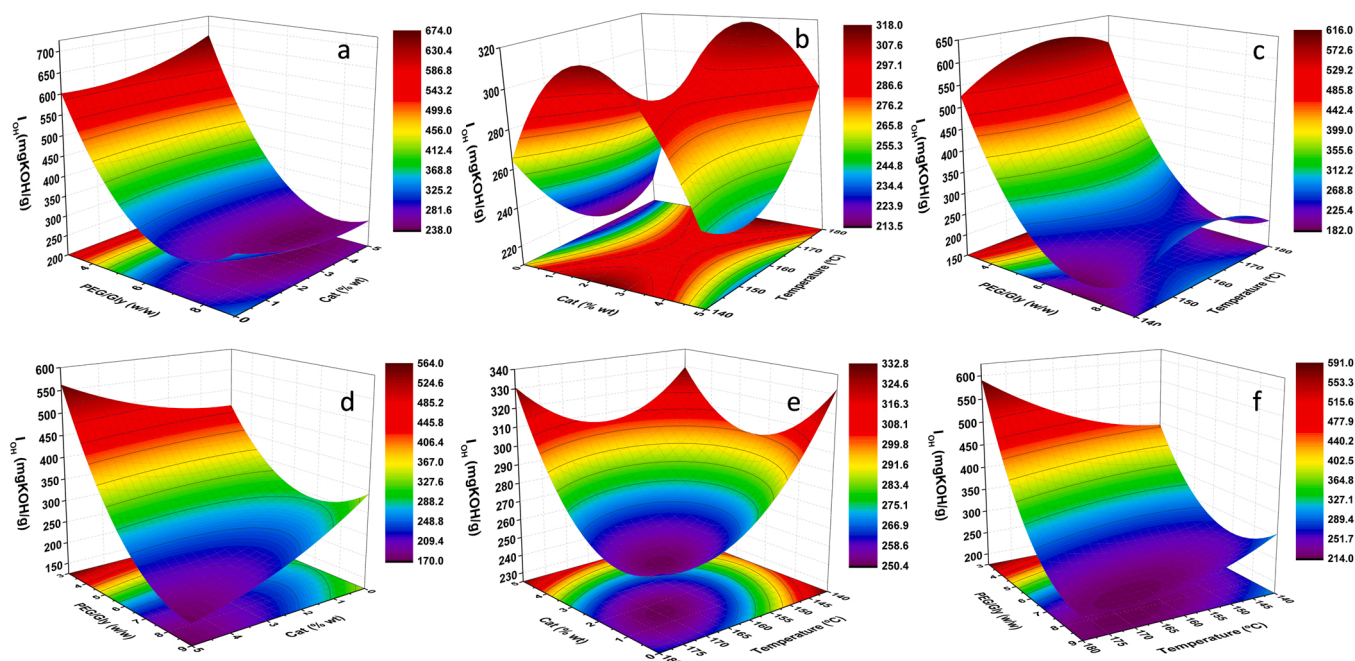


Fig. 5. Response surface for  $I_{OH}$ : *Eucalyptus globulus* (a, b, c); *Pinus radiata* (d, e, f).

molecular weight in the case of the bio-polyol obtained from *Eucalyptus globulus*, while in the case of the bio-polyol from *Pinus radiata* it was the independent variable catalyst concentration  $X_1$ , the interaction  $X_{23}$  and the quadratic effect of  $X_{11}$ . On the other hand, the independent variables that demonstrated a significant relevance for the  $I_{OH}$  were the effect of the PEG/Gly ( $X_3$ ) and the quadratic effects  $X_{22}$  and  $X_{33}$  for the bio-polyol obtained from *Eucalyptus globulus*, whereas for the bio-polyol from *Pinus radiata* only the independent variables catalyst concentration ( $X_1$ ) and temperature ( $X_2$ ) did not show a significant effect, while the remaining variables were significantly relevant.

### 3.2.1. Average molecular weight ( $M_w$ )

Fig. 4 shows the influence of the independent variables as well as their interactions on the molecular weight of bio-polyols obtained through the liquefaction of *Eucalyptus globulus* (4a, 4b and 4c) and *Pinus radiata* (4d, 4e and 4f).

Fig. 4a and d represent the response surfaces in which the interaction effect between the independent variables  $X_1$  and  $X_3$  is shown. As is evident in both figures, the independent variable  $X_3$  had almost no influence on the response ( $M_w$ ). On the other hand, in both cases, an increment in the concentration of the catalyst increased the molecular weight of the obtained bio-polyols. It should be noted in Fig. 4d that, for the bio-polyols that were obtained from the liquefaction of lignin from *Pinus radiata*, the maximum value of  $M_w$  was obtained for a catalyst concentration between 4% and 4.5%, after which the molecular weight decreased as the concentration increased. This behaviour could be explained by the influence of the quadratic term of the catalyst ( $X_{11}$ ) on the molecular weight equation.

The influence of the independent variables  $X_1$  and  $X_2$  and their interaction on the molecular weight for a fixed value of the independent variable  $X_3$  is shown in Fig. 4b and e. In both cases, an increase of the catalyst concentration ( $X_1$ ) and the temperature ( $X_2$ ) resulted in an increase of the molecular weight of the bio-polyols. As can be seen, the bio-polyol from the liquefaction of *Eucalyptus globulus* lignin reached the maximum molecular weight at one of the extremes of the design T (180°C) and Cat (5%). On the other hand, the bio-polyol from *Pinus radiata* lignin reached its maximum value of  $M_w$  for a catalyst concentration around 4% and decreased from this point as the concentration increased due to the quadratic effect of the independent variable ( $X_1$ ) on

the molecular weight equation. As for temperature, the highest  $M_w$  was obtained for a temperature of 175°C and decreased as the temperature increased above this point, although the quadratic term  $X_{22}$  was not significantly relevant (Table 4).

Fig. 4c and f show the response surface of  $M_w$  in function of temperature and PEG/Gly for a fixed value of concentration ( $X_1 = 0$ ). According to the regression coefficients summarised in Table 4, the molecular weight of the bio-polyol from *Eucalyptus globulus* was not affected by the independent variable PEG/Gly whilst the influence of the temperature was significantly relevant. This is evident from Fig. 4c, where it can be observed that a variation on the temperature had a significant impact on the molecular weight of the bio-polyol, whereas the PEG/Gly had little influence on the molecular weight regardless of the reaction temperature. On the other hand, in the case of bio-polyol from the liquefaction of lignin from *Pinus radiata* (Fig. 4f), neither the independent variable temperature nor PEG/Gly had a relevant significance in the molecular weight equation, although the interaction between both ( $X_{23}$ ) proved to be significantly relevant. In Fig. 4f, it can be noticed that the molecular weight of the bio-polyols is favoured by a high temperature and low PEG/Gly, obtaining the maximum when the temperature was at its highest (180°C) and the PEG/Gly was at its lowest, that is, at one of the extremes of the design.

One explanation for the high influence of the independent variables  $X_1$  and  $X_2$  on the  $M_w$ , could be that lignin during the microwave liquefaction process first degrades into small fragments that react with polyhydric alcohols (polyethylene glycol and glycerol) via ether bonds. Nevertheless, in the presence of catalyst and elevated temperatures, these lignin fragments can repolymerise, resulting in larger molecules and thus increasing the molecular weight (Hu et al., 2014; Xue et al., 2015).

### 3.2.2. Hydroxyl number ( $I_{OH}$ )

The influence of the independent variables and their interactions upon  $I_{OH}$  of the liquefied bio-polyols are shown in Figs. 5a, 5b and 5c (*Eucalyptus globulus*) and 5d, 5e and 5f (*Pinus radiata*).

For a fixed value of the temperature ( $X_2 = 0$ ), the influence of the independent variables  $X_1$  and  $X_3$  as well as the interactions between them are shown in Fig. 5a and d. As mentioned above, the independent variable  $X_1$  did not show significant influence on the  $I_{OH}$  of the bio-

**Table 5**

Not normalised and normalised values of the optimal points.

Origin	Independent variables	Rigid bio-polyol		Elastic bio-polyol	
		Not-normalised	Normalised	Not-normalised	Normalised
<i>Eucalyptus globulus</i>	X <sub>1</sub>	-1	0.00	1	5.00
	X <sub>2</sub>	0.0479	161	1	180
	X <sub>3</sub>	-1	3.00	0.5246	7.57
<i>Pinus radiata</i>	X <sub>1</sub>	-1	0.00	0.5430	3.86
	X <sub>2</sub>	-0.0456	159	0.0066	160
	X <sub>3</sub>	-1	3.00	0.4466	7.34

polyols regardless the used raw material. On the other hand, the independent variable X<sub>3</sub> exhibited a significant influence in both cases, as indicated in Table 4. This behaviour is illustrated in the response surfaces curves. In both cases, an increase in the ratio resulted in a reduction of the hydroxyl number, whereas increasing the amount of glycerol in the mixture, i.e., reducing the PEG/Gly, drastically increased the hydroxyl number. It should be noted that, although the catalyst was not significantly influential, both the maximum and minimum hydroxyl value of the bio-polyols were obtained by using high concentrations of catalyst.

The response surfaces 4b and 4e were obtained by fixing the independent variable X<sub>3</sub> to 0. Fig. 5b present a saddle point as a critical point, which means that the equilibrium is an inflection point between a relative maximum and a relative minimum. Therefore, this point does not serve as an optimal value. However, it is possible to identify the optimal region by visual observation of the surface (Bezerra et al., 2008). Thus, to maximise the I<sub>OH</sub>, a high temperature (180°C) and a catalyst concentration around 3.5% is preferable, while the minimum I<sub>OH</sub> value was obtained employing a reaction temperature around 170°C without catalyst. On the other hand, a clear minimum I<sub>OH</sub> value at 170°C and a catalyst concentration of 1.5% was observed in the case of the bio-polyol obtained from the liquefaction of *Pinus radiata* lignin (Fig. 5e).

Finally, the response surfaces corresponding to the interaction of the independent variables temperature (X<sub>2</sub>) and PEG/Gly (X<sub>3</sub>), as well as their interactions, for a fixed value of X<sub>1</sub> = 0 are plotted in Fig. 5c and f. Similarly, to Fig. 5a and d, it is possible to appreciate the great influence of the independent variable X<sub>3</sub> on the I<sub>OH</sub>. Thus, a lower PEG/Gly implied an increase in the I<sub>OH</sub>, while a higher ratio resulted in a decrease of the hydroxyl number of the bio-polyols. Therefore, a minimum of hydroxyls was obtained for a PEG/Gly of almost 9 at a temperature of 170°C in the case of bio-polyol from the liquefaction of *Pinus radiata* lignin (Fig. 5f). On the other hand, the response surface corresponding to the liquefaction of *Eucalyptus globulus* lignin (Fig. 5c) exhibited a saddle point. In this case, the maximum I<sub>OH</sub> was obtained for a temperature of 165°C and a maximum PEG/Gly (3), whereas the minimum I<sub>OH</sub> corresponded to the maximum temperature (180°C) and a PEG/Gly close to 8.

From the regression data summarised in Table 4 and the response surfaces, it can be noticed that the independent variable X<sub>3</sub> had the largest influence on the I<sub>OH</sub>. This is due to the fact that polyethylene glycol has a lower number of free hydroxyls than glycerol, and therefore, as the amount of PEG increases with respect to glycerol, the hydroxyl number of the polyol decreases (Jin et al., 2011).

### 3.2.3. Optimisation and model validation

The aim of the optimisation was to determine the optimal reaction conditions for the synthesis of bio-polyols suitable for the manufacture of rigid and elastic polyurethanes. To do that, the desirability function of the Statgraphic Centurion XVI software was employed. In the optimisation of the bio-polyol conditions for the synthesis for rigid polyurethanes, the objective was to minimise the molecular weight while increasing the hydroxyl groups, whereas the opposite was sought for the optimisation of reaction conditions in the case of elastic polyurethane bio-polyols, i.e., an increase in the molecular weight of the bio-polyols

**Table 6**Theoretical values of M<sub>w</sub> and corrected I<sub>OH</sub> predicted by the software and experimental values at optimum conditions.

Parameter	Sample	Theoretical value	Experimental value
M <sub>w</sub> (g/mol)	EPR <sup>a</sup>	1532	1394 ± 12
	EPE <sup>b</sup>	5593	4895 ± 325
	PPR <sup>c</sup>	1372	1383 ± 43
	PPE <sup>d</sup>	4891	5408 ± 765
I <sub>OH</sub> (mg KOH/g)	EPR	599	595 ± 34
	EPE	221	254 ± 61
	PPR	456	514 ± 43
	PPE	212	210 ± 4

<sup>a</sup> EPR (*Eucalyptus globulus* Organosolv Polyols for Rigid PU)

<sup>b</sup> PPR (*Pinus radiata* Organosolv Polyol for Rigid PU)

<sup>c</sup> EPE (*Eucalyptus globulus* Organosolv Polyol for Elastic PU)

<sup>d</sup> PPE (*Pinus radiata* Organosolv Polyol for Elastic PU)

while reducing the hydroxyl groups (Ionescu, 2019). The optimised reaction settings for the above-mentioned bio-polyols are summarised in Table 5, where the not-normalised and the normalised values of the independent variables are included as well.

To verify the model, a triplicate of each experiment was performed under the optimal reaction conditions and the experimental results were compared with the theoretical results presented in Table 6. As a result of this comparison, it was established that the experimental results were in good concordance with the data predicted by the software, and therefore, the Box-Behnken design was validated.

### 3.2.4. Characterisation of the optimised bio-polyols

In reference to the molecular weight (Table 6), it should be noted that, as indicated in the previous Section (3.2.1), an increase in the catalyst concentration resulted in an increase in the molecular weight of the bio-polyols. Hence, EPE and PPE bio-polyols presented higher M<sub>w</sub> than EPR and PPR bio-polyols in which no catalyst was used. In addition, the molecular weights of EPE and PPE bio-polyols were higher than the ones of the employed lignins, EUL and PUL respectively, in contrast to the reports of other authors. Thus, in the study by da Silva and dos Santos (2017) for the optimal liquefaction conditions of Kraft lignin, authors reported smaller molecular weights than the employed Kraft lignin for all points of the experimental design. In another study, da Silva et al. (2019) proved that the molecular weights of the bio-polyols obtained by liquefaction employing organic acids as catalyst were lower than the molecular weights of the Kraft lignin used. Similarly, Xue et al. (2015) also obtained bio-polyols through liquefaction reactions with lower molecular weights than the ones of the employed original lignin using a catalyst concentration of 1.5%. The increase in molecular weight can be explained as the repolymerisation reactions of lignin are favoured by the presence of acid catalyst (Lee and Lee, 2016). On the other hand, a concentration of sulphuric acid over 3% could enhance the repolymerisation reactions of lignin (Hu et al., 2014). According to the literature, the molecular weight of polyols for rigid and elastic PU should be between 300 and 1000 (g/mol) and 2000–10000 (g/mol), respectively (Ionescu, 2019). Considering the obtained results, although the molecular weights of EPR and PPR bio-polyols were slightly above the

**Table 7**

$M_n$  (g/mol), PDI ( $M_w/M_n$ ),  $A_n$  (mg KOH/g), functionality ( $f$ ) and yield (%) of bio-polyols at optimum conditions.

Sample	$M_n$ (g/mol)	PDI ( $M_w/M_n$ )	$A_n$ (mg KOH/g)	$f$	Yield (%)
EPR	$380 \pm 7$	$3.69 \pm 0.08$	$2.74 \pm 0.00$	$4.03 \pm 0.15$	$98.63 \pm 0.71$
EPE	$524 \pm 28$	$9.37 \pm 1.12$	$33.01 \pm 0.00$	$2.36 \pm 0.44$	$71.98 \pm 1.41$
PPR	$387 \pm 4$	$3.58 \pm 0.08$	$5.36 \pm 0.23$	$3.55 \pm 0.26$	$98.93 \pm 0.10$
PPE	$778 \pm 7$	$6.95 \pm 0.91$	$30.56 \pm 0.15$	$2.91 \pm 0.08$	$87.56 \pm 3.30$

stipulated range, it could be considered that the obtained bio-polyols are suitable for PU fabrication.

Regarding the  $I_{OH}$  of the studied bio-polyols, EPR and PPR showed higher values than EPE and PPE. This increment could be explained by two main reasons: firstly, an increase in catalyst concentration could decrease the hydroxyl number of the bio-polyol (Jin et al., 2011) and secondly, an increase in glycerol content, with a higher number of free hydroxyl than PEG, could enhance the hydroxyl number of the final bio-polyol (Chen and Lu, 2009). According to the literature, bio-polyols for rigid PUs, EPR and PPR, are in the range of  $I_{OH}$  required for the manufacture of rigid PUs (200–1000 mg KOH/g). However, the bio-polyols EPE and PPE were slightly above the range of 28–160 mg KOH/g, which is the one required for the manufacture of elastic PU (Li et al., 2015b).

In the literature, most of the existing works are focused on two parameters: hydroxyl number and yield. Nevertheless, parameters such as the number average molecular weight ( $M_n$ ), PDI,  $A_n$  and  $f$  should be considered in the synthesis of polyols (Hernández-Ramos et al., 2021). Thus, although these parameters were not considered in the experimental design, they are summarised in Table 7 together with the obtained yield. Bio-polyols functionality ( $f$ ) and the liquefaction yield ( $\eta$ ) were calculated using the Eqs. 4 and 5:

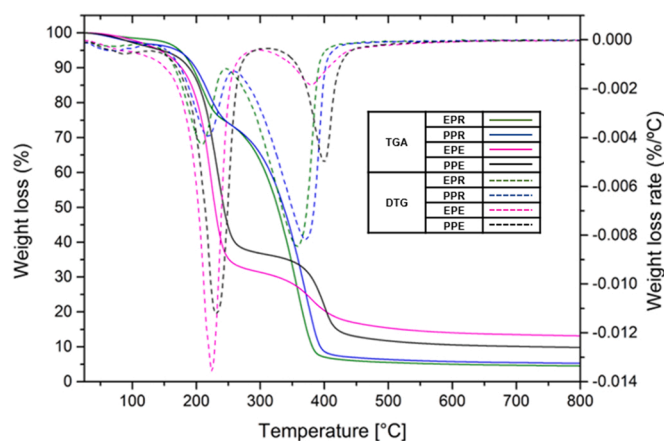
$$f = \frac{M_n \cdot I_{OH}}{1000 \cdot 56.1} \quad (4)$$

$$\eta = \frac{M}{M_0} \cdot 100 \quad (5)$$

Where,  $M$  is the final bio-polyol mass and  $M_0$  is the mass of the initial mixture of the liquefaction procedure.

The polydispersity index indicated that the EPE and PPE bio-polyols had wider molecular weight distribution than EPR and PPR bio-polyols. The reason for this could be due to a higher number of repolymerisation reactions in the synthesis of EPE and PPE bio-polyols, as discussed previously. Wider molecular weight distributions of EPE and PPE indicates that the chain length variability of these bio-polyols is higher than in EPR and PPR. This variability has a direct impact on the properties of the polyurethane, hence a bio-polyol with lower PDI is preferable for the manufacture of polyurethane foams, as a wide variability of the bio-polyol chain lengths could result in softening of the foam or in a mechanical collapse due to stresses that occur in the weaker regions of the foam (D'Souza et al., 2017).

In the synthesis of polyurethanes, the  $A_n$  value of bio-polyols is an important parameter to be considered, since acid groups could decrease the efficiency of the reaction (Hu and Li, 2014). According to the literature, the bio-polyols studied in this work showed an  $A_n$  index within the range reported by other authors, usually ranging from 0 to 40 mg KOH/g (Hu et al., 2014). As it can be seen in Table 7, those bio-polyols in which no catalyst was used (EPR and PPR) showed a lower  $A_n$  index than in the bio-polyols with higher acid concentration (EPE and PPE). This is because the number of acid substances generated during the liquefaction tended to increase, as the catalyst concentration increased (da Silva

**Fig. 6.** TGA thermograms and DTG curves of bio-polyols.

et al., 2019). Furthermore, as expected, the bio-polyols with the lowest acid number (EPR and PPR) showed the highest hydroxyl number, since there is a direct correlation between the increase of acid number and the decrease hydroxyl number (Lee et al., 2000).

Regarding functionality, to the best of our knowledge, no work has been reported indicating the functionality of polyols obtained by liquefaction of lignin with PEG and glycerol. A summary of the functionalities obtained in this study is presented in Table 7. Obtained values for EPR and PPR bio-polyols ( $4.03 \pm 0.15$  and  $3.55 \pm 0.26$ ), as well as for EPE and PPE bio-polyols ( $2.36 \pm 0.44$  and  $2.91 \pm 0.08$ ) are suitable for the synthesis of rigid and elastic PUs, whose functionalities should be between 3 and 8 and 2–3 (Ionescu, 2019).

Finally, as summarised in Table 7, significant differences were found in the obtained yields between the bio-polyols for rigid PUs and those for elastic PUs. Thus, the EPR and PPR bio-polyols showed quite similar yields between them,  $98.63 \pm 0.71\%$  and  $98.93 \pm 0.10\%$  respectively. These results are very similar to those published by other authors who used the same microwave liquefaction reaction time that was employed in this work. For instance, da Silva and dos Santos (2017) documented a yield of 95.27% for the liquefaction of Kraft lignin using 3% catalyst, while Sequeiros et al. (2013) obtained yields over 94% for all points of their experimental design employing organosolv lignin from olive pruning. Xue et al. (2015) liquefied alkaline lignin from corn cob waste applying a catalyst concentration of 1.5% to obtain a yield of 94.47%. On the other hand, Gosz et al. (2018) obtained a yield of 93% by liquefying pine Kraft lignin with 1,4-butanediol and crude glycerol without catalyst. In contrast, EPE and PPE bio-polyols exhibited significantly lower yields,  $71.98 \pm 1.41\%$  and  $87.56 \pm 3.30\%$ . Two reasons could explain the large difference between the yields of bio-polyols for rigid PU (EPR and PPR) and bio-polyols for elastic PU (EPE and PPE). On the one hand, as mentioned above, an increase in the concentration of the acid catalyst enhances the lignin repolymerisation reactions, which increases the solid residue, leading to a reduction in the final yield. On the other hand, an excess of glycerol in the mixture promotes the reaction yield. This is because during the reaction the glycerol can be condensed into polyglycerol forming water as a by-product. Such water

**Table 8**

Main degradation stages on TGA-DTG analysis.

Sample	1st degradation stage		2nd degradation stage		3rd degradation stage	
	T interval (°C)	$T_{max}$ (°C)	T interval (°C)	$T_{max}$ (°C)	T interval (°C)	$T_{max}$ (°C)
EPR	40–120	70	130–246	208	246–417	356
PPR	40–120	68	132–260	218	260–430	371
EPE	40–120	78	135–293	225	293–452	380
PPE	40–120	80	139–298	230	298–452	399

**Table 9**

Power-Law Linear functions based on the rheological data from bio-polyol samples.

Sample	Function	$k$ (Pa·s <sup>n</sup> )	$n$	$r^2$
EPR	$\tau = 0.2623 \cdot \dot{\gamma}^{0.9709}$	0.2623	0.9709	0.9995
PPR	$\tau = 0.4394 \cdot \dot{\gamma}^{1.0043}$	0.4394	1.0043	0.9998
EPE	$\tau = 0.8137 \cdot \dot{\gamma}^{0.9541}$	0.8137	0.9541	0.9995
PPE	$\tau = 1.1885 \cdot \dot{\gamma}^{0.9525}$	1.1885	0.9525	0.9998

fragments the lignin into smaller and more reactive molecules through hydrolysis, enhancing the reaction yield (Gosz et al., 2018).

To analyse the relationship between chemical structure and degradation, the bio-polyols were subjected to a thermogravimetric analysis. The TGA thermograms and their corresponding DTG derivative thermogravimetric curves are presented in Fig. 6. Through the study of the DTG curves, three degradation stages were observed which are summarised in Table 8.

The first degradation stage corresponds to the weight loss of the humidity of the samples. The second degradation stage correspond to the degradation of glycerol (153–267 °C) and the third degradation stage corresponded to the degradation of PEG (267–392 °C) and lignin (Briones et al., 2012). Since lignin degradation takes place between 300 and 500°C, this third degradation region of bio-polyols reaches higher temperatures than if only PEG were present. It can be observed that, as the  $M_w$  of bio-polyols increases, the degradation temperature is delayed; moreover, the lower the reaction yield, the lower the weight loss. An explanation for this, is that the lower the yield, the higher the lignin repolymerisation reactions, which results in a greater solid residue and, therefore, a lower final amount of lignin in the bio-polyol. These results confirmed that the combination of the liquefying solvents and lignin was successful.

Finally, to determine the rheological behaviour of the bio-polyols, a rotational test was performed. Through this test, the relationship between viscosity ( $\eta$ ), shear stress ( $\tau$ ) and shear rate ( $\dot{\gamma}$ ), which were fitted to the Ostwald-de Waele (power-law) equation (Eq. 6), was studied to determine the bio-polyols' fluid behaviour as well as their viscosity.

$$\tau = k \cdot \dot{\gamma}^n \quad (6)$$

where  $n$  and  $k$  are adjustment parameters dependent on both the measurement conditions and the nature of the fluid. Depending on the value of the flow index parameter ( $n$ ) the fluid could be Newtonian when  $n = 1$ , pseudoplastic if  $n < 1$  and dilatant for  $n > 1$ . The parameter  $k$ , also called consistency index, which is associated to the apparent viscosity of the fluid at a shear rate of  $1 \text{ s}^{-1}$ , exhibits higher values as the viscosity increases. In Table 9 and Figs. 7a and 7b, a summary of the

data, obtained by the software and the flow curves, are presented.

The high values of  $r^2$  reported in Table 9 indicated that all the rheograms are well fitted. Therefore, it could be concluded that the selected model was adequate to evaluate the rheological behaviour of the bio-polyols. Considering that the flow index parameter ( $n$ ) of all bio-polyols is very close to unity, it could be concluded that all bio-polyols behave as Newtonian fluids. However, analysing the Fig. 7a, the rheograms corresponding to EPE and PPE showed a pseudoplastic behaviour, i.e., the viscosity ( $\eta$ ) decreased as the shear rate ( $\dot{\gamma}$ ) increased, while EPR and PPR bio-polyols exhibit a clearly Newtonian behaviour, where the viscosity remained constant regardless the applied shear rate. Fig. 7b, where the relationship between the shear stress ( $\tau$ ) and shear rate ( $\dot{\gamma}$ ) is represented, confirms that EPR and PPR bio-polyols behaved as Newtonian fluids since their graphical representation is a line passing through the origin, while the representation of EPE and PPE bio-polyols subtly exhibited the characteristic curve of pseudoplastics fluids, where  $\tau$  decreases as  $\dot{\gamma}$  increases.

It is well known that the power-law becomes Newton's Law when a fluid behaves in a Newtonian way and therefore the viscosity of the fluid corresponds to any point along the plateau in the Fig. 7a, i.e., the consistency index  $k$  is equal to the viscosity. Therefore, the viscosities for EPR and PPR are 0.2626 Pa·s and 0.4394 Pa·s respectively. On the other hand, the viscosities of EPE and PPE are in the range of 0.7286–0.6676 Pa·s and 1–0.9310 Pa·s respectively at the studied shear rate. As it was expected, since viscosity and molecular weight are closely related (da Silva and dos Santos (2017), the bio-polyols with the highest viscosities were those with the highest molecular weight. According to literature, this viscosities values are suitable for PU production since they are below 300 Pa·s (Cateto et al., 2009) and are similar to the viscosities obtained by other authors by liquefying lignin (Briones et al., 2012; da Silva et al., 2019, 2017; Xue et al., 2015).

#### 4. Conclusions

Through Box Behnken experimental design and employing response surface methodology, the optimal lignin liquefaction reaction conditions using microwave irradiation technology for obtaining bio-polyols to formulate rigid and elastic polyurethanes were obtained. Four optimum points were obtained, two of them for bio-polyols to produce rigid polyurethanes (EPR and PPR), and other two for bio-polyols to produce elastic polyurethanes (EPE and PPE). The high  $R^2$  determination coefficients obtained for the studied parameters ( $M_w$  and  $I_{OH}$ ) together with Fisher's F-test confirmed that the selected models were appropriate and that they were well adjusted. The optimum reaction conditions for EPR and PPR bio-polyols were virtually equals, around 160 °C and PEG/Gly ratio of 3, noteworthy is the absence of catalyst in both cases. On the

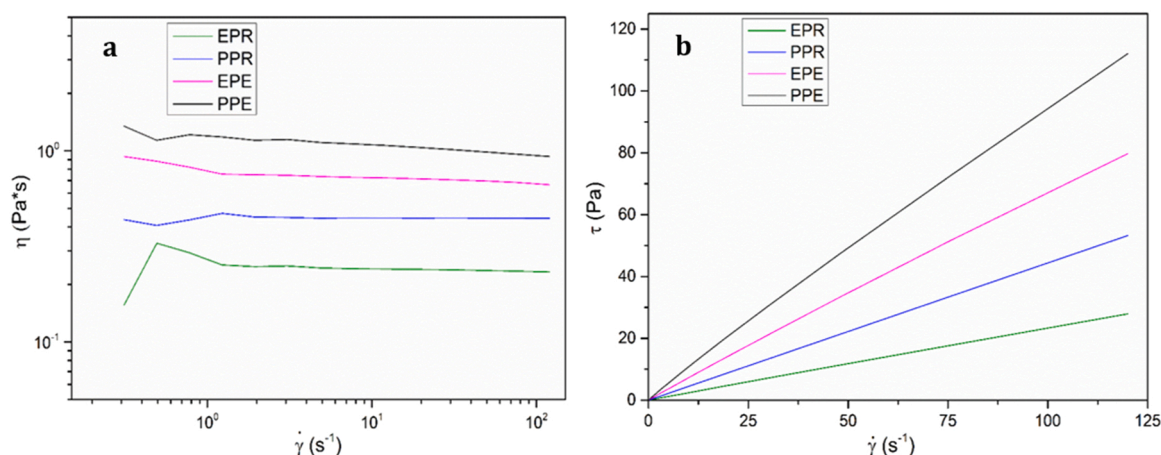


**Fig. 7.** (a) Viscosity ( $\eta$ ) VS shear rate ( $\dot{\gamma}$ ) and (b) shear stress ( $\tau$ ) VS shear rate ( $\dot{\gamma}$ ) of bio-polyols at optimum point.

other hand, the optimum reaction conditions were 180 °C and polyethylene glycol/glycerol ratio of 7.57 for EPE and 160 °C and polyethylene glycol/glycerol ratio of 7.34 for PPE. The high concentration of catalyst, 5.00% and 3.85% respectively, is remarkable in both cases. The molecular weight of EPR and PPR bio-polyols at the optimum points was slightly higher than that required for the manufacture of rigid polyurethanes. Similarly, the hydroxyl number of EPE and PPE bio-polyols was slightly higher than the required for the manufacture of elastic PUs. However, considering the rest of the studied parameters: acid number ( $A_n$ ), polydispersity index (PDI), functionality ( $f$ ) and the rheological behaviour, it could be concluded that the bio-polyols showed a great potential to be used in the synthesis of polyurethanes. Nevertheless, before their use, the bio-polyols should be neutralised due to the high acid number and for polyurethane foams preparation the high polydispersity should be taken into account.

### CRedit authorship contribution statement

**Fabio Hernández-Ramos:** Conceptualization, Methodology, Investigation, Formal analysis, Data curation, Validation, Writing – original draft, Writing – review & editing. **Vincent Novi:** Methodology, Investigation, Visualization. **María González Alriols:** Supervision, Validation, Data curation, Visualization. **Jalel Labidi:** Validation, Formal analysis, Resources, Supervision. **Xabier Erdocia:** Methodology, Investigation, Formal analysis, Data curation, Validation, Supervision, Writing – original draft, Writing – review & editing.

### Declaration of Competing Interest

The authors declare the following financial interests/personal relationships which may be considered as potential competing interests: Fabio Hernandez-Ramos reports financial support was provided by Gipuzkoa Provincial Council.

### Data Availability

Data will be made available on request.

### Acknowledgements

The authors would like to acknowledge the financial support of the University of the Basque Country (project COLAB20/04). F.Hernández-Ramos would like to acknowledge the Grant received from the Environmental Department of the Diputación Foral de Gipuzkoa. The authors thank SGiker (UPV/EHU/ERDF, EU) for their technical and human support.

### References

- ASTM, 2013. ASTM D974–12 Designation: Standard Test Method for Acid and Base Number by Color-Indicator Titration 1 i, 1–7. <https://doi.org/10.1520/D0974-12.2>.
- Bezerra, M.A., Santelli, R.E., Oliveira, E.P., Villar, L.S., Escalera, L.A., 2008. Response surface methodology (RSM) as a tool for optimization in analytical chemistry. *Talanta* 76, 965–977. <https://doi.org/10.1016/j.talanta.2008.05.019>.
- Briones, R., Serrano, L., Labidi, J., 2012. Valorization of some lignocellulosic agro-industrial residues to obtain biopolyols. *J. Chem. Technol. Biotechnol.* 87, 244–249. <https://doi.org/10.1002/jctb.2706>.
- Cateto, C.A., Barreiro, M.F., Rodrigues, A.E., Belgacem, M.N., 2009. Optimization study of lignin oxypropylation in view of the preparation of polyurethane rigid foams. *Ind. Eng. Chem. Res.* 48, 2583–2589. <https://doi.org/10.1021/ie801251r>.
- Chen, F., Lu, Z., 2009. Liquefaction of wheat straw and preparation of rigid polyurethane foam from the liquefaction products. *J. Appl. Polym. Sci.* 111, 508–516. <https://doi.org/10.1002/app.29107>.
- Chen, L., Wang, X., Yang, H., Lu, Q., Li, D., Yang, Q., Chen, H., 2015. Study on pyrolysis behaviors of non-woody lignins with TG-FTIR and Py-GC/MS. *J. Anal. Appl. Pyrolysis* 113, 499–507. <https://doi.org/10.1016/j.jaap.2015.03.018>.
- Cinelli, P., Anguillesi, I., Lazzeri, A., 2013. Green synthesis of flexible polyurethane foams from liquefied lignin. *Eur. Polym. J.* 49, 1174–1184. <https://doi.org/10.1016/j.eurpolymj.2013.04.005>.

- D'Souza, J., Camargo, R., Yan, N., 2017. Biomass liquefaction and alkoxylation: a review of structural characterization methods for bio-based polyols. *Polym. Rev.* 57, 668–694. <https://doi.org/10.1080/15583724.2017.1283328>.
- da Silva, S.H.F., dos Santos, P.S.B., Thomas da Silva, D., Briones, R., Gatto, D.A., Labidi, J., 2017. Kraft lignin-based polyols by microwave: optimizing reaction conditions. *J. Wood Chem. Technol.* 37, 343–358. <https://doi.org/10.1080/02773813.2017.1303513>.
- da Silva, S.H.F., Egiús, I., Labidi, J., 2019. Liquefaction of Kraft lignin using polyhydric alcohols and organic acids as catalysts for sustainable polyols production. *Ind. Crop. Prod.* 137, 687–693. <https://doi.org/10.1016/j.indcrop.2019.05.075>.
- Erdocia, X., Prado, R., Corcuera, M.Á., Labidi, J., 2014. Base catalyzed depolymerization of lignin: Influence of organosolv lignin nature. *Biomass Bioenergy* 66, 379–386. <https://doi.org/10.1016/j.biombioe.2014.03.021>.
- Erdocia, X., Hernández-ramos, F., Morales, A., Izaguirre, N., Hoyos-martínez, P.L., De, Labidi, J., 2021. Lignin extraction and isolation methods. In: *Lignin-Based Materials for Biomedical Applications*. Elsevier Inc, pp. 61–104. <https://doi.org/10.1016/c2019-0-01345-3>.
- Fernández-Marín, R., Hernández-Ramos, F., Salaberria, A.M., Andrés, M.Á., Labidi, J., Fernandes, S.C.M., 2021. Eco-friendly isolation and characterization of nanochitin from different origins by microwave irradiation: optimization using response surface methodology. *Int. J. Biol. Macromol.* 186, 218–226. <https://doi.org/10.1016/j.ijbiomac.2021.07.048>.
- Gómez-Jiménez-Aberasturi, O., Ochoa-Gómez, J.R., 2017. New approaches to producing polyols from biomass. *J. Chem. Technol. Biotechnol.* 92, 705–711. <https://doi.org/10.1002/jctb.5149>.
- Gomez-Lopez, A., Panchireddy, S., Grignard, B., Calvo, I., Jerome, C., Detrembleur, C., Sardon, H., 2021. Poly(hydroxyurethane) adhesives and coatings: state-of-the-art and future directions. *ACS Sustain. Chem. Eng.* 9, 9541–9562. <https://doi.org/10.1021/acssuschemeng.1c02558>.
- Gosz, K., Kosmela, P., Hejna, A., Gajowicz, G., Piszczyk, L., 2018. Biopolyols obtained via microwave-assisted liquefaction of lignin: structure, rheological, physical and thermal properties. *Wood Sci. Technol.* 52, 599–617. <https://doi.org/10.1007/s00226-018-0991-4>.
- Hai, T.A.P., Tessman, M., Neelakantan, N., Samoylov, A.A., Ito, Y., Rajput, B.S., Pourahmady, N., Burkart, M.D., 2021. Renewable polyurethanes from sustainable biological precursors. *Biomacromolecules* 22, 1770–1794. <https://doi.org/10.1021/acsbio.0c01610>.
- Hernández-Ramos, F., Alriols, M.G., Calvo-Correas, T., Labidi, J., Erdocia, X., 2021. Renewable biopolyols from residual aqueous phase resulting after lignin precipitation. *ACS Sustain. Chem. Eng.* <https://doi.org/10.1021/acssuschemeng.0c09357>.
- Hu, S., Li, Y., 2014. Polyols and polyurethane foams from base-catalyzed liquefaction of lignocellulosic biomass by crude glycerol: effects of crude glycerol impurities. *Ind. Crop. Prod.* 57, 188–194. <https://doi.org/10.1016/j.indcrop.2014.03.032>.
- Hu, S., Luo, X., Li, Y., 2014. Polyols and polyurethanes from the liquefaction of lignocellulosic biomass. *ChemSusChem* 7, 66–72. <https://doi.org/10.1002/cssc.201300760>.
- Ionescu, M., 2019. Polyols, in: De Gruyter (Ed.), *Polyols for Polyurethanes*. Berlin, pp. 1–10. <https://doi.org/10.1515/9783110644104-001>.
- Jin, Y., Ruan, X., Cheng, X., Lü, Q., 2011. Liquefaction of lignin by polyethyleneglycol and glycerol. *Bioresour. Technol.* 102, 3581–3583. <https://doi.org/10.1016/j.biortech.2010.10.050>.
- Kühnel, I., Podschun, J., Saake, B., Lehnen, R., 2015. Synthesis of lignin polyols via oxyalkylation with propylene carbonate. *Holzforschung* 69, 531–538. <https://doi.org/10.1515/hf-2014-0068>.
- Lambeth, R.H., 2021. Progress in hybrid non-isocyanate polyurethanes. *Polym. Int.* 70, 696–700. <https://doi.org/10.1002/pi.6078>.
- Laurichesse, S., Avérous, L., 2014. Chemical modification of lignins: towards biobased polymers. *Prog. Polym. Sci.* 39, 1266–1290. <https://doi.org/10.1016/j.progpolymsci.2013.11.004>.
- Lee, S.H., Yoshioka, M., Shiraiishi, N., 2000. Liquefaction of corn bran (CB) in the presence of alcohols and preparation of polyurethane foam from its liquefied polyol. *J. Appl. Polym. Sci.* 78, 319–325. [https://doi.org/10.1002/1097-4628\(20001010\)78:2<319::AID-APP120>3.0.CO;2-Z](https://doi.org/10.1002/1097-4628(20001010)78:2<319::AID-APP120>3.0.CO;2-Z).
- Lee, Y., Lee, E.Y., 2016. Liquefaction of red pine wood, *pinus densiflora*, biomass using peg-400-blended crude glycerol for biopolyol and biopolyurethane production. *J. Wood Chem. Technol.* 36, 353–364. <https://doi.org/10.1080/02773813.2016.1156132>.
- Li, Y.Y., Luo, X., Hu, S., 2015a. Lignocellulosic biomass-based polyols for polyurethane applications. *Bio-Based Polyols Polyurethanes* 1–79. <https://doi.org/10.1007/978-3-319-21539-6>.
- Li, Y.Y., Luo, X., Hu, S., 2015b. Introduction to bio-based polyols and polyurethanes. *Bio-Based Polyols Polyurethanes* 1–79. <https://doi.org/10.1007/978-3-319-21539-6>.
- Methods, S.T., 2000. Standard test methods for polyurethane raw materials: determination of unsaturation. Test 08, 3–6. <https://doi.org/10.1520/D4671-05.2>.
- Morales, A., Gullón, B., Dávila, I., Eibes, G., Labidi, J., Gullón, P., 2018. Optimization of alkaline pretreatment for the co-production of biopolymer lignin and bioethanol from chestnut shells following a biorefinery approach. *Ind. Crop. Prod.* 124, 582–592. <https://doi.org/10.1016/j.indcrop.2018.08.032>.
- Nde, D.B., Barekati-Goudarzi, M., Muley, P.D., Khachatryan, L., Boldor, D., 2021. Microwave-assisted lignin liquefaction in hydrazine and ethylene glycol: Reaction pathways via response surface methodology. *Sustain. Mater. Technol.* 27, e00245 <https://doi.org/10.1016/j.susmat.2020.e00245>.
- Perez-Arce, J., Centeno-Pedraza, A., Labidi, J., Ochoa-Gómez, J.R., García-Suarez, E.J., 2020. A novel and efficient approach to obtain lignin-based polyols with potential

- industrial applications. *Polym. Chem.* 11, 7362–7369. <https://doi.org/10.1039/d0py01142h>.
- Sequeiros, A., Serrano, L., Briones, R., Labidi, J., 2013. Lignin liquefaction under microwave heating. *J. Appl. Polym. Sci.* 130, 3292–3298. <https://doi.org/10.1002/app.39577>.
- Tran, M.H., Yu, J.H., Lee, E.Y., 2021. Microwave-assisted two-step liquefaction of acetone-soluble lignin of silvergrass saccharification residue for production of biopolyol and biopolyurethane. *Polymers* 13. <https://doi.org/10.3390/polym13091491>.
- Wells, T., Kosa, M., Ragauskas, A.J., 2013. Polymerization of Kraft lignin via ultrasonication for high-molecular-weight applications. *Ultrason. Sonochem.* 20, 1463–1469. <https://doi.org/10.1016/j.ultsonch.2013.05.001>.
- Xue, B.L., Wen, J.L., Sun, R.C., 2015. Producing lignin-based polyols through microwave-assisted liquefaction for rigid polyurethane foam production. *Materials* 8, 586–599. <https://doi.org/10.3390/ma8020586>.